

EMplifier: Hybrid Electromagnetic Probe for Side Channel and Fault Injection Analysis

Fabrizia Marrucco, Mosabbah Mushir Ahmed, Bechir Bouali and Alieeldin Mady
Qualcomm Technologies, Cork, Ireland

Keywords: Hardware Security, Offensive Security, EM-FI, SCA.

Abstract: Electromagnetic Fault Injection (EM-FI) analysis is increasingly emerging as an effective technique to bypass countermeasure and/or leak sensitive information by injecting fault during the execution of sensitive asset/operation. EM-FI analysis becomes an essential requirement for obtaining product security certification, whenever high assurance is claimed. The coils represent an integral part of the EM probe design. Therefore, it is important to focus on the practical study of coil design that accentuate the efficiency of EM capture and emission. In this work we tried to optimize the design of a hybrid coil (called *EMplifier*) that can efficiently sense the EM emissions and inject the fault, enabling a guided fault injection analysis with a single coil. This state-of-art investigates the various important coil parameters that can be used in a hybrid scenario of both capturing and emitting EM signals. Such design is useful in practical EM-FI setup where identifying the exact injection location over the chip is a key factor towards successful attacks.

1 INTRODUCTION

High security assurance is rapidly becoming an industrial requirement for assets connected to internet, ranging from smart garage door openers, smart home locks, smart TVs, and handsets to automobiles. These connected Internet-of-things (IoT) and Cyber-Physical Systems (CPS) link together devices that were previously isolated, where critical application and infrastructure enforce the high assurance security requirements (Li et al., 2016).

Providing high security assurance starts by building a highly resilient hardware, which acts as a root of trust for software components on top (Mansour & Lauf, 2020). Hardware is produced in a mass-production with a static security footprint, where a successful attack on a single device can lead to reducing resiliency of applications use this hardware. Software patching has an easier process than hardware in case of vulnerability identification, hence industry has been enforcing a high security assurance requirement for security critical application, such as banking, payment terminals, passport. Common Criteria certification (CC) scheme (Common Criteria, 2022) was introduced to formulate a security evaluation standardization by levelling the security assurance level using

Evaluation Assurance Level (EAL). CC scheme has introduced a disruptive change in the industrial landscape, where hardware security requirements were benchmarked against the application domain used by this hardware, e.g., passport and banking applications require EAL7 to reflect the maximum assurance level.

Hardware security evaluation considers two main attack categories: Side-Channel Analysis (SCA) and Fault injection (FI) attacks. Side-channel analysis (Koeune & Standaert, 2005) aims to extract secrets/keys from chips through measuring and analysing hardware physical parameters, such as power consumption, response time, and EM emission. Fault injection analysis (Barengi et al., 2012) aims to gain privileges or extract secrets/keys by modifying the device execution flow by injecting faults using different medium, such as voltage/clock glitching, body-biasing (BBI), EM-FI and laser emissions (L-FI).

EM-FI, BBI and L-FI are classified as localised-FI attacks, where fault is precisely injected on the die's backside to perturbate targeted asset in isolation of the surrounded subsystems/assets. The isolation nature of the localised-FI leads to a high precision and effective perturbation, which increasingly emerges as a common method in evaluating System-On-Chip (SoC) security resiliency. Within localised-FI, EM-FI

has gained a significant recognition by offensive security community due to the attack cost efficient, where an optimal compromise is achieved between attack cost versus effectiveness (Barengi et al., 2012; Dehbaoui et al., 2012).

Developing EM-FI attack follows multiple stages, where identifying the optimal injection location over the die is a key stage towards a successful attack. Typically, side-channel EM leakage is useful to identify the optimal location of the injection, based on the maximum leakage location for the targeted assets. Even though EM medium is used for both side channel leakage and fault injection, two different probes will be required with manual switching. Passive EM sensing probe is used to evaluate the EM leakage, whereas fault is injected by active EM probe. Switching between these two probes is challenging due to the required micrometre scale precision needed. The use of an XYZ table can help in obtaining an approximate location but doesn't allow us to have a high precision.

While certain studies have investigated into optimizing the design of EMFI coils and others have focused on enhancing sensing coils designs, no prior research has attempted to identify an optimal design that consider both aspects. In this work our primary focus has been on developing a hybrid coil, called *EMplifier*, where *EMplifier* aims to efficiently monitor EM emission (i.e., passive EM-probe) and inject EM signal (i.e., active EM-probe).

Although the probe for both SCA and FI requires certain amount circuit elements like amplifier, switches, pulse generator etc., the design of other parts of the probes is not in the scope of this work. The main contributions are manifold, listed as follows:

- Comprehension of design parameters of the probe that affect the FI and SCA capability.
- Design of a novel hybrid EM-probe coils, enabling multi-stage FI attack.
- Experimental study for optimising *EMplifier* design parameters.

2 RELATED WORKS

We can identify two types of EM-FI platforms. The single probe type requires two different probes used for passive and active operations. The dual EM-probe, proposed in this paper, is used to perform EM injections and side-channel measurements.

Regarding the design of EM-FI probes several research have been conducted. For instance, in (Gaine

et al., 2022) the characteristics of EM-probe to increase the effectiveness of the EM injection while limiting the requirement of high voltages has been studied. The key characteristics are selecting a soft high permeability ferrite for probe's core and overlaying the probe coil turns. Moreover, ChipShouter (*NAE-CW520*, n.d.) is widely used EMFI platform in hardware research community. The tool can generate up to 500 V. The probes provided with the tool are 1 mm or 4 mm in diameter. The core is made of ferrite. Also, SiliconToaster (Abdellatif & Heriveaux, 2020) is a custom EM-FI platform. The tool can produce a pulse of 1200 V. The EM probe used with SiliconToaster is built from a flat coil of 6.6 mm diameter with 9 turns. The core is made of ferrite with a 4.5 mm diameter and 10 mm length. Despite this, the only commercial solution capable of injecting EM pulses and performing EM measurement simultaneously using the same probe is the EM-FI Transient Probe with Adjustable Pulse Width (EM-FI Transient Probe Adjustable Pulse Width - Riscure, n.d.) that can generate up to 100 V (power over coil). Nevertheless, no public details related to characteristics of the probe design have been published.

In comparison to the related studies, this work focusses on the fundamental aspects of EM probe i.e., the coil. A thorough investigation is made to understand the important characteristics of the coil pertaining to both FI and SCA. Furthermore, in comparison to this existing hybrid commercial design (EM-FI Transient Probe Adjustable Pulse Width - Riscure, n.d.), this work investigates the coil aspect of the EM-FI probe, whereas the existing commercial tools do not give the explicit detail of the different aspects of the probe that contributes to the hybrid nature. On the other hand, in applications where precise location of the EM emission is needed can be achieved by recording the XYZ co-ordinate, but such an architecture still requires changing the probes manually that can be expensive in terms of time and mechanical adjustments/errors. *EMplifier* design can inhibit the use of such multiple probe settings.

3 PRELIMINARIES

The two main aspects that determines the operation of the EM probe coils are:

- EM interaction mechanisms
- Field region

First, the coupling laws are based on Biot-Savart's law and Faraday's law. The first is a

fundamental quantitative relationship between an electric current I and the magnetic flux B that it produces. This law is the basis of the phenomenon whereby, having obtained a current through the coil, it generates a magnetic field proportional to the current that generated it. The generated magnetic field can then generate an induced current according to the well-known Faraday's law (Kinsler, 2020; Oliveira & Miranda, 2001). These laws are applicable for both SCA (also referred as signal sensing in this paper) and FIA (fault injection attacks).

Secondly, the field of interest for this work and in general FI and SCA testing is the near-field region. This region has complex characteristic and approximations rules. Consequently, obtaining accurate simulation is particularly complex (Nikitin et al., 2007) and changes in the design of the coils can significantly affect its efficiency in terms of FIA and SCA. Moreover, is not possible to have a complete control over all the parameters that will affect the FIA success rate or the SCA sensitivity.

3.1 Parameters Characteristics

Utilizing the aspects or features stated above, a set of parameters are selected that are utilized for the effective design of the EM probes. The design of the probe is categorized into two parts: (1) selection of parameters, (2) design and test. For the first part, parameters are classified under certain sub-categories - independent parameters set (*IPS*) and dependent parameter set (*DPS*). The characteristic of the *IPS* is that they consist of variables that can be controlled while designing the probe. This set of parameters could include dimensions of the solenoid, the spacing between the coils, the number of turns, and the material used. The outcome of *IPS* decides the *DPS*. Some of the *DPS* observed during the EM probe design and testing are the signal amplitude, resonant frequency, sensitivity etc.

Due to the complexity of simulating the interaction between the EM coil and the DUT, it is not possible to show with high precision how changing the values of the *IPS* will affect all the *DPS* values. Therefore, before going into the design phase, a procedure has been conducted and can be summarize with the Algorithm 1. This procedure has the aim of evaluating if the values chosen for the *IPS* will make the *DPS* values correspond with the expected requirements, 'test_req' in the Algorithm 1. Due to the hybrid nature of the EM probe, it is necessary that the choice of *IPS* is significant for both SCA and FIA or, in other words, that *IPS(FI)* and *IPS(SCA)* have interjection.

A list of important sets of *DPS* and *IPS* taken into consideration while designing the probe are highlighted in Table 1. Observing from Table 1, *IPS* are approximately common for both SCA and FIA although the *DPS* can vary. Therefore, this interjection is decisive in the choice of design parameters as they will correspond to the common *IPS*.

3.2 DPS Parameters Brief

In this section, some of the important *DPS* that are critical to be understood for the design of hybrid coil, are briefly discussed.

Damping of the Injected Current. Ideally for FI it is better to have a critically damped response refer that will result in a value that can be approximated as in (1) if the circuit can ideally be represented as an RLC circuit (Beckers et al., 2020), as shown in:

$$I = \frac{V_0}{L} t \exp\left(\frac{-R}{2L}t\right) \quad (1)$$

here, I is the current, V_0 is the initial voltage, R and L are resistance and inductor respectively (Dannehl et al., 2011). Over-damping would increase the pulse-width, while under-damping results in ringing. The amount of coupling between the probe and the device itself changes with the frequency of the EM pulse.

Coupling. Different frequencies can result in different values of coupling effecting the induced current and overall system behaviour. This frequency dependency complicates the study and comprehension of the EM-pulse injection process.

Directivity. It measures the concentration of the radiation pattern of the probe in a particular direction. A higher directivity indicates a better focus and signal-to-noise ratio (SNR) values of the field / signals. It applies to both FI and SC equally. This makes it less sensitive to noise (or signals) coming from other directions or sources.

Algorithm 1: Selection of parameters.

1. **procedure:** Calculate DPS Decide $IPS(test_req)$:
 2. **select** the test requirements 'test_req'
 3. **check** if $DPS = test_req$ |
 4. **if** test_req meets certain conditions:
 5. $DPS = calculate_DPS_based_on_test_req$
 6. **if** criteria_for_DPS_are_fulfilled(DPS):
 7. $IPS = make_decision_based_on_DPS(DPS)$
 8. **else**
 9. **reset** IPS
 10. **end procedure**
-

Table 1: Parameters example list for the probe design.

| Parameter | Variables |
|------------------|--------------------------------------------------------------------------------------|
| <i>DPS (SCA)</i> | Signal-to-noise ratio (SNR), Directivity, Coupling between DUT and probe |
| <i>IPS (SCA)</i> | No. of turns, Type of core, Diameter of the coil |
| <i>DPS (FI)</i> | Power of the injected EM field, Coupling between DUT and probe, Directivity, Damping |
| <i>IPS (FI)</i> | No. of turns, Type of core, Diameter of the coil |

4 EMPLIFIER DESIGN

The efficiency of a hybrid EM probe's coil is determined by some important parameters that define the limitations and range of its working frequency, power etc. Those independent values, the *IPS* effects *DPS* values and are the one we can control when designing the probe. From the selection phase and the requirements (*test_req* from Algorithm 1), several important aspects (that can be part of *IPS*) have been identified. These are also illustrated in Figure 1.

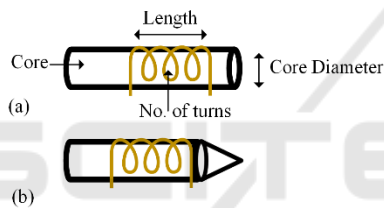


Figure 1: Different *IPS* sets used during the design of the hybrid EM-probe. (a) Flat shape (b) Sharp-tip.

4.1 Number of Turns (N)

Number of turns (N) is an important characteristic of the probes, changing its value effects both FI and SC capability. In one the first studies on the N required for FI, it is shown, with the help of simulation results, that only a single loop (turn) would be sufficient however (Omarouyache et al., 2013), as research progressed in this area, it has been observed that one loop does not seem to be the most effective solution in the case of FI (Ordas et al., 2017).

As an important aspect for FI, the goal is not to generate the highest magnetic field amplitude, but to preferably maximize the rate of change of H -field at the rising and falling edges of the pulse as it will affect the induced current value. When the number of windings increases, the inductance (L) is expected to rise quadratically with the number of windings (Beckers et al., 2020).

$$L = \frac{k\mu_0 N^2 A}{l} \quad (2)$$

From (2), $k\mu_0$ determines the material properties – magnetic permeability, the other part of equation $N^2 A/l$ shows the geometrical characteristics – number of turns, area, length of solenoid respectively. Going back to (2) it can be observed that with increased L , the current (I) decreases, but at the same time it impacts positively for the B refer to (3), where R is the parameter that determines the radius of the core (solenoid).

$$B = \frac{k\mu_0 NI}{2l} \left[\frac{1}{R} \right] \quad (3)$$

In general, it could be possible to assume that if N increases, under certain limits, the two effects will slightly compensate each other (Caciagli et al., 2018). Also, damping of the circuit depends on L , the time window of the interaction between the EM pulse and circuit also is determined by multitude of the parameters and one of them is the N . In the case of under-damped condition, there can be number of harmonics that can further cause chain of faults (or multiple faults), the under-damped condition can be achieved by increasing the time-window of interaction which in turn depends upon N .

Regarding the value of N used for the SCA, in general a single loop with a variable gap size is used. On the other hand, as pointed out in (2) a high L value of the coil, at any frequency, is necessary because it increases the SNR and sensitivity for eddy-current testing. Resorting to Algorithm 1, for selection of *IPS* values (in this case N), empirical approaches are used recursively, using equations discussed above. Once the empirical approach sets the required *test_req*, the *DPS* obtained can be said to satisfy the requirements. Taking into considerations all the parameters and equations involved, and the previous research about FI, after some initial characterization, the N used in this study is between 4-7. The differences in the results for each N value is highlighted in section 5.

Similar approach has been used in deciding the core, length of solenoid and probe shape i.e. make use of Algorithm 1 and intersection of *IPS* and *DPS* parameters.

4.2 Choice of Core (Air vs Ferrite)

The core of the probe can be filled with a ferromagnetic element like ferrite or just left with air as core. There are various discussions on the pros and cons ferrite core can have. The main purpose of a magnetic core is to provide a convenient path for flux, enabling flux linkage or coupling (*DPS*) between multiple elements. The magnetic flux produced by the coil prefers to flow through the ferrite rather than

through the air. Consequently, the ferrite core concentrates the magnetic field near the centre of the probe, which in turn concentrates the eddy currents in that region. Referring to (W. Zhu et al., 2011) the cores acts as the flux linkage path between the circuit winding and a non-magnetic gap that is connected to the core. Such properties are very much useful for the FI technique.

For SCA part, ferrite core can work like a ferrite rod antenna that is a small magnetic loop antenna used in RFID applications. It is designed with a rod made of ferrites and includes a coil wound around it (D. Giri. 1977). The use of ferrite helps in channelizing the EM mission into the probe, thus reducing the noise (better directivity and SNR) coming from other sources. Hence in this work it has been found that filling a ferrite core is more advantageous for both SCA and FI with empirical results.

4.3 Shape of Probe

From previous studies it has been deduced that the best shapes for the EM probe for FI are - flat, crescent, and sharp (Chusseau, L et. al., 2014). The flat shape is widely used, however the sharp shape has shown very good results as it allows for better spatial resolution since the diameter of the tip is much smaller than in the flat shape, while still maintaining a high inductance value. This concentration is expected to enhance the accuracy and precision of the spatial resolution, making it more directive (*DPS*). The crescent shape is to create a circular magnetic field that is intentionally concentrated between the two ends of the ferrite (Trabelsi et al., 2019). This design aims to minimize magnetic pollution and interference within the space that separates the two ends of the ferrite.

Table 2: Summary of hybrid EM probes.

| Probe name | Shape | Diameter(mm) | No. of turns | Core Type |
|------------|-------|--------------|--------------|-----------|
| R1 | Flat | 2 | 4 | Ferrite |
| R2 | Flat | 3 | 4 | Ferrite |
| G1 | Flat | 2 | 7 | Ferrite |
| G2 | Flat | 3 | 7 | Ferrite |
| P1 | Sharp | 5 | 7 | Ferrite |
| P2 | Sharp | 2 | 7 | Ferrite |

For the SCA part, the focus is to localize the field through probe shape. The probe shape like flat and sharp have been characterized and tested for SCA because these shapes aid in capturing the radiation pattern while have good inductance value. Therefore, this work uses flat and sharp-tip probes.

4.4 Length of Solenoid

In terms of FI, decreasing the length of the solenoid has the positive effect of increasing the value of the inductance refer (2) and (3). There are two strategies which can be employed. Either the wire thickness can be reduced, or windings can be overlapped. For the SCA part, is important to take in account that longer coils result in a reduction of coupling (*DPS*) between source and pick-up coils. A longer coil will also mean a lower inductance value and a worse SNR.

4.5 Coil Architecture

Based upon the investigation of different parameters a list of coils designed using such is given in Table 2. The coils in this table are consequence of cumulating parameters that forms part of *IPS* and *DPS* for both SCA and FI applications. A correlation with the designed coil and different parameters described are also highlighted in Figure 1.

5 EXPERIMENTAL DESIGNS

Based on the conjunction of all the parameter sets, experiments are carried out. The experiments highlight the efficiency of various probes designed with parameters determined above. Also, a Figure-of-merit is discussed that shows the effects of various parameters involved in the design of an efficient hybrid-EM probe.

The coils are designed using the study carried out in previous sections (also refer Table 2). Since not much information can be found about the use of ferrite probes with copper windings in the side-channel case, the number of turns is chosen within a range of {4-7}, following the indication obtain from the previous research in terms of FI efficiency. For similar reasons, the diameter of the core is fixed in a range of {2-5mm}. In all the cases, the two ends of the wire are soldered to an SMA connector. This connects the probe to the pulse generator, in the FI setup, and to the preamplifier, in the SCA setup. Execution of both FI and SCA experiments are divided into experimental setup and testing phase.

5.1 Execution of FI

First part of experiment is the execution of FI on the selected DUT and observe it results. The details of experiment and results are given below.

5.1.1 Setup for FI

A typical setup to perform the EM-FI, consists of a pulse generator, an XYZ table, and software to orchestrate all components, as is shown in Figure. 2(a). For all the produced probes the position and the distance from the DUT has been fixed to be able to compare them.

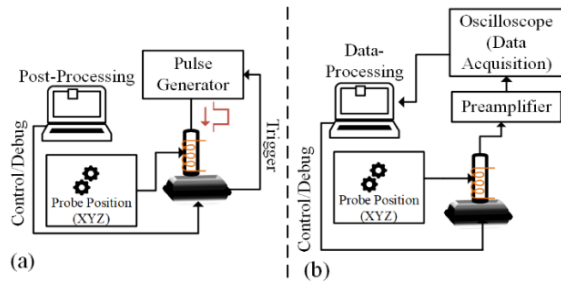


Figure 2: A typical setup for experiments. (a) EM-FI. (b) EM-SCA.

In this work ChipSHOUTER from newAE®, has been used for pulse generation. This device can generate one or multiple pulses in a range from 150 to 500V with a pulse-width from 80 to 960ns. Fundamentally, the ChipSHOUTER provides a high voltage charge that is discharged through an inductor (EM probe), that generates a powerful magnetic field that can be used to induce faults in a target device (Dehbaoui et al., 2012; NAE-CW520, n.d.). Pulses can be triggered by internal or external trigger logic. The DUT in this work has been an Arduino Mega2560, based on the 8-bit AVR microcontroller ATmega2560. This target has been chosen over other available MCUs, like the Arduino UNO, because of his thinner package, that makes the penetration of the EM through the package easier, without requiring any decapsulation. The pulse generator has been mounted on a XYZ table that allows to move the EMFI probe to the attack location. Faults injected by EM fields are location dependent.

5.1.2 Testing Phase

For the FI experiment, a counter loop test program is used to evaluate possible number of injected faults each of the built probes (refer Table 2). A serial communication is used that establishes the trigger the start of test program.

Using a Python script, the PC establishes a serial connection also with the ChipSHOUTER from newAE® and reset both the devices. An internal trigger is used, that is programmed and set by initial characterization. The pulse voltage value used in this

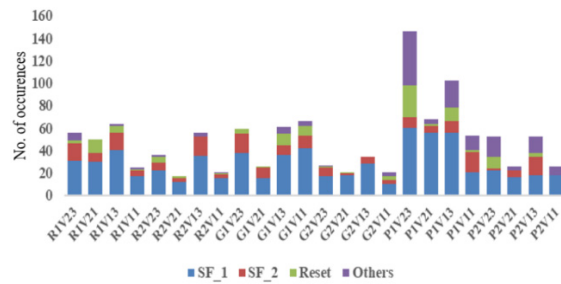


Figure 3: FI results from different types of probes.

work are 350 and 450V termed as $V1$ and $V2$ respectively. The delay from trigger is set at 200ms obtained after initial characterization. The pulses repetition is between 1 and 3.

For every designed EM probe, 250 pulses have been injected to see how many faults it is possible to obtain. The expected value of the counter is 25000, so values like 25001 and 24999 have been taken as successful faults termed as SF_1 and SF_2 respectively. Every other obtained value is considered under *others* category. Moreover, the number of resets occurred is taken in account. There are six probes designed refer Table 2. For the FI part each probe has classifications or groups based on voltage and repetition rates. There are 24 configurations of probes tested for the FI part. Each probe, voltage level and repetition rate are grouped under one configuration for better understanding of results. For instance, $RIV11$ corresponds to probe RI , voltage used is 350V ($V1$) and the repetition is 1. The result for the FI part with all the probe is shown in Figure 3. Referring Figure. 3, it is not straightforward to precisely find which of the coil is the best among all, however using approximate result from Figure. 3, it can be deduced that for flathead GI and sharp-edge PI have yielded better results. The choice depends on the DUT type, testing environment, algorithm type etc.

5.2 Execution of SCA

In the second part of the experiment, the coils are tested to evaluate their ability to sense the EM emissions. The setup for the SCA part is depicted in Figure. 2(b). Here a pre-amplifier is used which is used that enhances the SNR of the EM emission sensed by the probes. In this work PA306 from Langer has been as a low noise preamplifier. Also in this case, during the first characterization, a side-channel commercial probe has been used to identify a spot where the emission where easily detected and this spot has been used to compare all the built probes,

kept at direct contact with the DUT. The DUT is, also in this case, the Arduino MEGA-2560, but the test algorithm is AES-128, a symmetric key cryptographic algorithm. It is done so, because EM emission from loop counter algorithm is not easily distinguishable, whereas for AES-128 (Dehbaoui et al., 2012), the EM emission characteristic is well-known, and it is convenient to detect that on the DUT used here also. Like FI, for SCA probe is moved in XYZ direction and spot in decide from where maximum emission is observed.

For more analytical analysis, an FFT has been applied to the sensed signal to evaluate the gain (in dBm) at the fundamental frequency of 16MHz, that is equal to the clock frequency of the Arduino Mega, as shown in the Figure 4. From the result in Table 3, it is observed that for both *NF*-based and FFT calculation, the *G1* and *P1* seems to show better results. Although empirically *NF*-based solution helps to observe signal analysis in the time domain, the result for sensing a signal is more accurately be considered in the frequency domain. The results from Figure 4 and Table 3, suggests that coils *G1* and *P1* are suitable hybrid EM probe. But this is applicable for the DUT used in this work. The results highly depend upon DUT, test platform, algorithm etc.

Table 3: Results of emission for different probes.

| Probes | G1 | G2 | R1 | R2 | P1 | P2 |
|-----------|-------|-------|-------|-------|-------|-------|
| FFT (dBm) | -4.51 | -7.12 | -6.02 | -9.64 | -6.66 | -6.01 |
| NF (mV) | 508.4 | 495.3 | 376.9 | 490.9 | 541.2 | 531.6 |

5.3 Figure-of-Merit

As seen from the above results, when using such a hybrid-EM probe, a trade-off is needed to meet the requirements for SCA and FIA. In this case, an empirical formula has been proposed in (4):

$$FM = k_r \frac{N}{l} \left(\frac{1}{D1} \right) + \frac{D1}{D2} \tag{4}$$

where, k_r is magnetic permeability, N is no. turns, $D1$ and $D2$ are diameters of the core refer Figure 5. The expression obtained considers how the *IPS* and the *DPS* values will correspond to the test requirements (*test req*).

The $(D1/D2)$ factor has been added to consider the shape of the tip. This suggests empirically that the bigger the FM value is, the better the trade-off between sensing and injecting capability is.

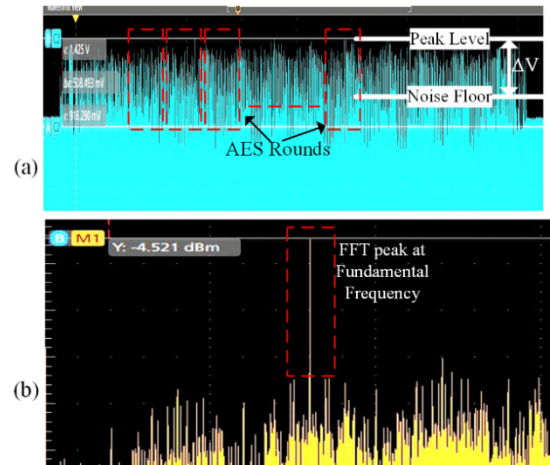


Figure 4: EM emission observed from hybrid probe. (a) AES rounds with Noise Floor approach. (b) FFT of AES emission.

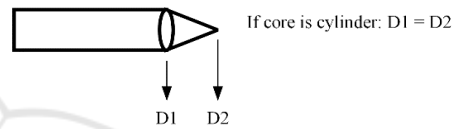


Figure 5: A basic geometry of flathead and sharp-tip probe.

6 CONCLUSION

In this paper a thorough study has been conducted on characteristics and parameters of EM coil. Using this study, a novel hybrid nature of EM coil has been designed, and subsequently a figure-of-merit is proposed. The experiments conducted on FI and SCA parts highlights that the designed hybrid coils can sense and emit the EM signals to/from the DUTs. The experimental results showcase that such designs can enable a novel guidance-based EM-FI techniques, significantly increasing the EM-FI effectiveness, while reducing the attack model cost and complexity. As a future effort, the EM probe setting will be evaluated against lower nano-meter tech nodes.

REFERENCES

Abdellatif, K. M., & Heriveaux, O. (2020). SiliconToaster: A Cheap and Programmable EM Injector for Extracting Secrets. *2020 Workshop on Fault Detection and Tolerance in Cryptography (FDTC)*, 35–40. <https://doi.org/10.1109/FDTC51366.2020.00012>.

Barengi, A., Breveglieri, L., Koren, I., & Naccache, D. (2012). *Fault Injection Attacks on Cryptographic Devices: Theory, Practice, and Countermeasures*.

- Proceedings of the IEEE, 100(11), 3056–3076. <https://doi.org/10.1109/JPROC.2012.2188769>.
- Beckers, A., Kinugawa, M., Hayashi, Y., Fujimoto, D., Balasch, J., Gierlichs, B., & Verbauwhe, I. (2020). *Design Considerations for EM Pulse Fault Injection* (pp. 176–192). https://doi.org/10.1007/978-3-030-42068-0_11.
- Caciagli, A., Baars, R. J., Philipse, A. P., & Kuipers, B. W. M. (2018). Exact expression for the magnetic field of a finite cylinder with arbitrary uniform magnetization. *Journal of Magnetism and Magnetic Materials*, 456, 423–432. <https://doi.org/10.1016/j.jmmm.2018.02.003>
- Chusseau, L., Omarouyache, R., Raoult, J., Jarrix, S., Maurine, P., Tobich, K., Bover, A., Vrignon, B., Shepherd, J., Le, T.-H., Berthier, M., Riviere, L., Robisson, B., & Ribotta, A.-L. (2014). Electromagnetic analysis, deciphering and reverse engineering of integrated circuits (E-MATA HARI). *2014 22nd International Conference on Very Large Scale Integration (VLSI-SoC)*, 1–6. <https://doi.org/10.1109/VLSI-SoC.2014.7004189>.
- Common Criteria. 2022. *Common Methodology for Information Technology Security Evaluation*.
- Dannehl, J., Liserre, M., & Fuchs, F. W. (2011). Filter-Based Active Damping of Voltage Source Converters With LCL Filter. *IEEE Transactions on Industrial Electronics*, 58(8), 3623–3633. <https://doi.org/10.1109/TIE.2010.2081952>.
- Dehbaoui, A., Dutertre, J.-M., Robisson, B., & Tria, A. (2012). Electromagnetic Transient Faults Injection on a Hardware and a Software Implementations of AES. *2012 Workshop on Fault Diagnosis and Tolerance in Cryptography*, 7–15. <https://doi.org/10.1109/FDTC.2012.15>.
- EM-FI Transient Probe Adjustable Pulse Width - Riscure. (n.d.). Retrieved September 13, 2023, from <https://www.riscure.com/em-fi-transient-probe-apw/>
- Gainé, C., Nikolovski, J.-P., Aboukassimi, D., & Dutertre, J.-M. (2022). New Probe Design for Hardware Characterization by ElectroMagnetic Fault Injection. *2022 International Symposium on Electromagnetic Compatibility – EMC Europe*, 299–304. <https://doi.org/10.1109/EMCEurope51680.2022.9901104>.
- Giri, D., King, R., & Wu, T. (n.d.). A theoretical and experimental study of the ferrite rod antenna. *1977 Antennas and Propagation Society International Symposium*, 242–245. <https://doi.org/10.1109/APS.1977.1147716>.
- Kinsler, P. (2020). Faraday's Law and Magnetic Induction: Cause and Effect, Experiment and Theory. *Physics*, 2(2), 148–161. <https://doi.org/10.3390/physics2020009>.
- Koene, F., & Standaert, F.-X. (2005). *A Tutorial on Physical Security and Side-Channel Attacks* (pp. 78–108). https://doi.org/10.1007/11554578_3.
- Li, H., Xing, J., & Ma, J. (2016). A high-assurance trust model for digital community control system based on internet of things. *Wuhan University Journal of Natural Sciences*, 21(1), 29–36. <https://doi.org/10.1007/s11859-016-1135-z>.
- Mansour, S., & Lauf, A. (2020). Hardware Root Of Trust for IoT Security In Smart Home Systems. *2020 IEEE 17th Annual Consumer Communications & Networking Conference (CCNC)*, 1–2. <https://doi.org/10.1109/CCNC46108.2020.9045412>.
- NAE-CW520. (n.d.). Retrieved September 13, 2023, from <https://www.newae.com/products/NAE-CW520>.
- Nikitin, P., Rao, K. V. S., & Lazar, S. (2007). An Overview of Near Field UHF RFID. *2007 IEEE International Conference on RFID*, 167–174. <https://doi.org/10.1109/RFID.2007.346165>.
- Oliveira, M. H., & Miranda, J. A. (2001). Biot-Savart-like law in electrostatics. *European Journal of Physics*, 22(1), 31–38. <https://doi.org/10.1088/0143-0807/22/1/304>.
- Omarouyache, R., Raoult, J., Jarrix, S., Chusseau, L., & Maurine, P. (2013). Magnetic microprobe design for EM fault attack. *2013 International Symposium on Electromagnetic Compatibility*, 949–954.
- Ordas, S., Guillaume-Sage, L., & Maurine, P. (2017). Electromagnetic fault injection: the curse of flip-flops. *Journal of Cryptographic Engineering*, 7(3), 183–197. <https://doi.org/10.1007/s13389-016-0128-3>.
- Trabelsi, O., Sauvage, L., & Danger, J.-L. (2019). *Characterization at Logical Level of Magnetic Injection Probes*. 625–628. <https://doi.org/10.23919/EMCTokyo.2019.8893692>.
- Zhu, W., Yin, W., Peyton, A., & Ploegaert, H. (2011). Modelling and experimental study of an electromagnetic sensor with an H-shaped ferrite core used for monitoring the hot transformation of steel in an industrial environment. *NDT & E International*, 44(7), 547–552. <https://doi.org/10.1016/j.ndteint.2011.05.005>.